

PROPERTIES OF $\text{Al}_2\text{O}_3/\text{TiO}_2$ AND ZrO_2/CaO FLAME-SPRAYED COATINGS

LASTNOSTI PLAMENSKO NANEŠENIH PREMAZOV $\text{Al}_2\text{O}_3/\text{TiO}_2$ IN ZrO_2/CaO

Artur Czupryński

Silesian University of Technology, Faculty of Mechanical Engineering, The Welding Department,
Konarskiego 18A, 44-100 Gliwice, Poland
artur.czuprynski@polsl.pl

Prejem rokopisa – received: 2015-07-01; sprejem za objavo – accepted for publication: 2016-02-09

doi:10.17222/mit.2015.165

The article presents the results of a study on the exploitation properties of flame-sprayed ceramic coatings produced from an oxide ceramic material in the form of powder based on an aluminum oxide (Al_2O_3) matrix with an addition of 3 % titanium oxide (TiO_2) and also on a zirconium oxide (ZrO_2) matrix with 30 % of calcium oxide (CaO) on a substrate of unalloyed structural steel of grade S235JR. The buffer layer was produced from a metallic powder on the basis of Ni-Al-Mo. Plates with dimensions of ($5 \times 200 \times 300$) mm and also the front surfaces of $\phi 40 \times 50$ mm cylinders were flame-sprayed. The buffer coatings were produced using a RotoTec 80 torch and external specific coatings were produced with a CastoDyn DS 8000 torch. Investigations of the coating properties were based on metallography tests, a phase-composition research, a measurement of microhardness, a research of the coating adhesion to the substrate, the abrasive-wear resistance (acc. to ASTM G65 standard), the erosion-wear resistance (acc. to ASTM G76-95 standard) and a thermal-stroke study. The coatings were characterized by a high adhesion to the substrate and also high erosion and abrasive-wear resistance and the resistance to cyclic thermal strokes.

Keywords: flame spray, coating, ceramic powder, abrasive-wear resistance, erosion-wear resistance, adhesion strength

Članek predstavlja rezultate študija uporabnih lastnosti plamensko nanešenih keramičnih premazov, izdelanih iz materiala oksidne keramike v obliki prahov na osnovi aluminijevega oksida Al_2O_3 z dodatkom 3 % titanovega oksida TiO_2 in tudi na osnovi cirkonovega oksida (ZrO_2) s 30 % kalcijevega oksida (CaO) na podlagi iz nelegiranega konstrukcijskega jekla S235JR. Tamponska plast je bila izdelana s kovinskim prahom na osnovi Ni-Al-Mo. Plošča dimenzij $5 \text{ mm} \times 200 \text{ mm} \times 300 \text{ mm}$ in tudi čelna stran površine valjev $\phi 40 \text{ mm} \times 50 \text{ mm}$ sta bili plamensko nanešeni. Tamponski nanos je bil izdelan z gorilnikom RotoTec 80, zunanji specifični nanos z gorilnikom CastoDyn DS 8000. Preiskave lastnosti nanosov so bile izvršene z metalografijo, preiskavo sestave faz, meritvijo mikrotrdote, preiskavo prijemljivosti nanosa na podlago, z preizkusom odpornosti na abrazijsko obrabo, (v skladu z ASTM G65 standardom), odpornost na erozijsko obrabo, (v skladu z ASTM G76-95 standardom) in s preizkusom na termošok. Značilnost nanosov je bila velika oprijemljivost na podlago, tudi odpornost na erozijsko in abrazijsko obrabo ter odpornost na toplotne šoke.

Ključne besede: plamensko nanašanje, nanos, keramični prah, odpornost na abrazijsko obrabo, odpornost na erozijsko obrabo, adhezijska trdnost

1 INTRODUCTION

Thermal-spraying methods have developed significantly in the recent years by applying more and more technically advanced heat sources and new coating materials.¹⁻¹⁰ At present, this technology is used in about 70 % of industrial applications for manufacturing new parts or devices, for which high-quality workmanship and appropriate surface properties are required. An improvement in the operating parameters of machine and equipment parts associated with high loads and speeds, causing accelerated wear and the necessity of an effective regeneration, also contributed to the rapid advancement in the thermal-spraying technology.

The application of flame-sprayed coatings has not only been conducive to multifold enhancement in the durability of the protection of steel structures against a corrosive environment, but has also led to an extended service life of textile machinery parts, cast moulds, rollers for steel-industry conveyors, parts of pumps and

stirrers, plastic-injection moulders, and has also improved the durability and reliability of power boilers.¹¹ Sprayed-ceramic coatings providing excellent thermal and electrical barriers have been manufactured more and more often due to high corrosion, erosion and wear resistance and hardness and high-temperature creep resistance. Ceramic-oxide materials based on aluminium oxide (Al_2O_3) and zirconium oxide (ZrO_2) are especially noteworthy. Thermal- and electric-barrier coatings flame-sprayed with such materials are applied in multiple cases, e.g., for electronic components, insulation parts of ignition plugs and power turbines, and high-temperature-resistant and heatstroke-resistant parts of combustion chambers in modern car and airplane engines.¹²⁻¹⁴

2 EXPERIMENTAL PROCEDURE AND RESULTS

The aim of the conducted investigations was to create technological conditions of flame powder spraying and

to compare the operating properties of ceramic coatings produced with Al_2O_3 - and ZrO_2 -based powders on the structural unalloyed S235JR steel acc. to EN 10025-2:2004. A powder with a content of 97 % of Al_2O_3 and 3 % of TiO_2 , and a powder with a content of 70 % of ZrO_2 and 30 % of CaO were selected for spraying. The binding powder (the buffer layer), i.e., a Ni-Al-Mo alloy, was employed as the primer coating.

Plates with dimensions of (5 × 200 × 300) mm and faces of $\phi 40 \times 50$ mm cylinders were subjected to a manual flame-spraying operation using the two aforementioned powders. Prior to the spraying process, the surfaces of the plates and cylinders were cleaned with shot blasting including an abrasive blasting treatment in conformity with the EN 13507:2010 requirements. Surface shot blasting was performed using angular particles of cast iron. The spraying process consisted of the following operations:

- a 50–100 μm primer coating (buffer layer) including the Ni-Al-Mo powder sprayed with a RotoTec 80 torch (**Table 1**);
- an approx. 500 μm external specific coating including the powder of 97 % Al_2O_3 + 3 % TiO_2 and the powder of 70 % ZrO_2 + 30 % CaO using a CastoDyn DS 8000 torch (**Table 2**).

Following the spraying process, the plates with ceramic coatings were cut into samples intended for further examinations. Adhesion tests of the coatings sprayed onto the substrates were performed on cylindrical samples. Metallographic macroscopic examinations of the sprayed surfaces were undertaken with a stereomicroscope with a magnification of 4–25 times.

Table 1: Spraying parameters of the primer coating with Ni-Al-Mo powder

Tabela 1: Parametri pri nanašanju podlage s prahom iz Ni-Al-Mo

| | |
|---|---------------------------|
| Torch type: | RotoTec 80 |
| Acetylene pressure: | 0.7 (bar) |
| Oxygen pressure: | 4.0 (bar) |
| Distance between the torch and the sprayed surface: | 200 (mm) |
| 12744 Preheating temperature: | 40 ($^{\circ}\text{C}$) |
| Change in the torch advancement angle relative to the next coating: | 90 $^{\circ}$ |

Table 2: Spraying parameters of the external coating with aluminium oxide and zirconium oxide matrices

Tabela 2: Parametri pri nanašanju zunanjskega nanosa z osnovo iz aluminijevega oksida in cirkonovega oksida

| | |
|---|--|
| Torch type: | CastoDyn DS 8000 |
| Torch tip: | SSM 30 |
| Powder flow rate: for 97 % Al_2O_3 + 3 % TiO_2 powder for 70 % ZrO_2 + 30 % CaO powder | 2 (setting acc. to the manual) 3 (setting acc. to the manual) |
| Acetylene pressure: | 0.7 (bar) |
| Oxygen pressure: | 4.0 (bar) |
| Assist. gas (compressed air) pressure: | 3.0 (bar) |

*The required primer coating made with Ni-Al-Mo powder

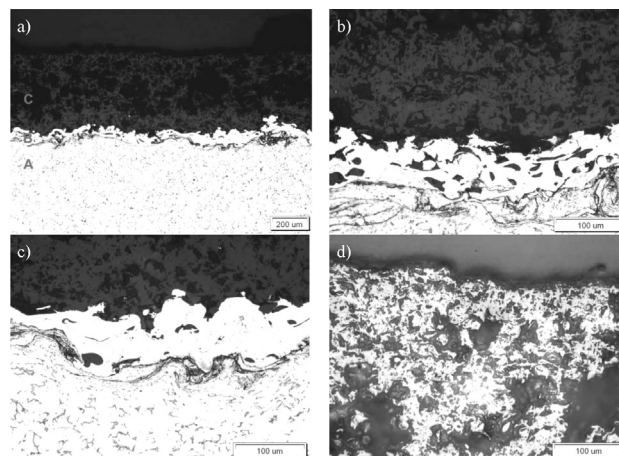


Figure 1: View after flame spraying with 97 % Al_2O_3 + 3 % TiO_2 powder: a) structure of specific external coating (C), primer Ni-Al-Mo coating (B) and base material (A), magn. of 100 \times ; b) structure of external coating and image of binding zone of external coating with primer coating, magn. of 400 \times ; c) structure of primer coating over the area of deformed steel with a developed surface line, magn. of 400 \times ; d) structure of external coating, magn. of 400 \times

Slika 1: Izgled plamensko nanešenega prahu s 97 % Al_2O_3 + 3 % TiO_2 : a) struktura posebnega zunanjskega nanosa (C), nanos podlage iz Ni-Al-Mo (B) in osnovno jeklo (A), povečava 100 \times ; b) struktura zunanjskega nanosa in slika vezivnega področja zunanjskega nanosa na vmesni nanos, povečava 400 \times ; c) struktura vmesnega nanosa na deformiranem jeklu z razvito linijo površine, povečava 400 \times ; d) struktura zunanjskega nanosa, povečava 400 \times

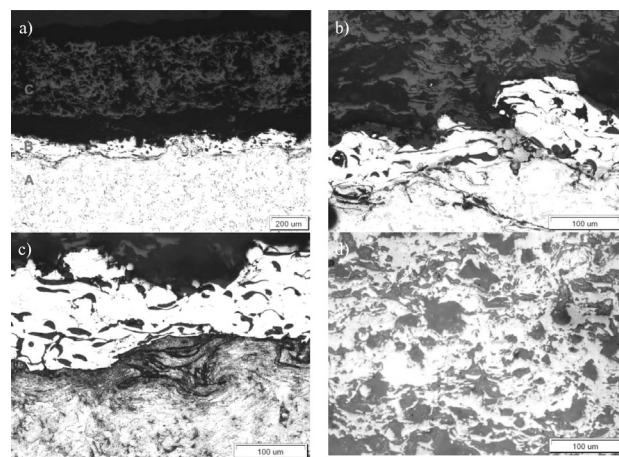


Figure 2: View after flame spraying with 70 % ZrO_2 + 30 % CaO powder: a) structure of specific external coating (C), primer Ni-Al-Mo coating (B) and base material (A), magn. of 100 \times ; b) structure of external coating with microhollows and image of binding zone of external coating with primer coating, magn. of 400 \times ; c) structure of primer coating over the area of deformed steel with a developed surface line, magn. of 400 \times ; d) structure of external coating, magn. of 400 \times

Slika 2: Izgled plamensko nanešenega prahu s 70 % ZrO_2 + 30 % CaO : a) struktura posebnega zunanjskega nanosa (C), nanos podlage iz Ni-Al-Mo (B) in osnovno jeklo (A), povečava 100 \times ; b) struktura zunanjskega nanosa z mikro prazninami in posnetek vezivnega področja zunanjskega nanosa z nanosom podlage, povečava 400 \times ; c) struktura nanosa podlage na deformiranem jeklu, z jasno linijo površine, povečava 400 \times ; d) struktura zunanjskega nanosa, povečava 400 \times

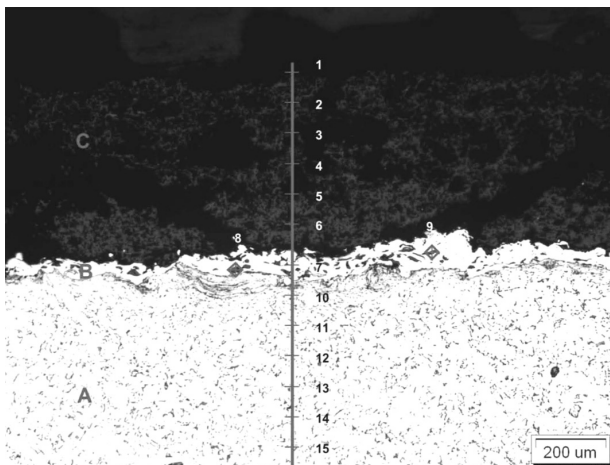


Figure 3: Diagram of hardness measurements at the cross-section of a sample after flame spraying: C – external specific coating, B – primer coating, A – substrate material

Slika 3: Prikaz meritve trdote na preseku vzorca po nanosu s plamenom: C – zunanji specifični premaz, B – nanos podlage, A – material osnove

Metallographic microscopic examinations were carried out on metallographic microsections perpendicular to the coating, cut from the plates after flame spraying with the powder matrix of aluminium oxide and zirconium oxide. The structure of the examined coatings was revealed on the microsections etched in a 4 % nitric acid solution (HNO₃) and ethyl alcohol solution (C₂H₅OH). Metallographic microscopic examinations were performed with a magnification of 100–1000×. The grain size in the plate structure was determined with the comparative method. The thickness of the coatings was determined with the metallographic method in compliance with ISO 1463 1997.

Table 3: Results of the hardness measurement on the cross-section of the sample after spraying it with 97 % Al₂O₃ + 3 % TiO₂ powder

Tabela 3: Rezultati meritve trdote na preseku vzorca po napršenem nanosu prahu s 97 % Al₂O₃ + 3 % TiO₂

| Test area | Test point | Load (N) | HV hardness |
|---|------------|----------|-------------|
| External coating (C) (97 % Al ₂ O ₃ + 3 % TiO ₂) | 1 | 5.0 | 747 |
| | 2 | 5.0 | 823 |
| | 3 | 5.0 | 910 |
| | 4 | 5.0 | 672 |
| | 5 | 5.0 | 762 |
| | 6 | 5.0 | 747 |
| Primer coating (B) (Ni-Al-Mo) | 7 | 0.1 | 469 |
| | 8 | 0.1 | 353 |
| | 9 | 0.1 | 458 |
| Substrate material (A) (S235JR) | 10 | 0.5 | 226 |
| | 11 | 0.5 | 189 |
| | 12 | 0.5 | 145 |
| | 13 | 0.5 | 131 |
| | 14 | 0.5 | 128 |
| | 15 | 0.5 | 110 |

Every result was represented by the average value of ten measurements. The results of the metallographic

microscopic examinations allowed us to evaluate the structure of the base material, the primer coating and the specific external coating and their thickness after the flame-spraying operation (Figures 1 and 2).

The coating-hardness measurement was made with the Vickers method. The examinations were carried out in conformity with ISO 6507-1:2007. The load applied during the hardness measurement was between 0.1 and 5 N. The hardness measurement was made at the cross-sections of the samples with the ceramic coatings including the powders of 97 % Al₂O₃ + 3 % TiO₂ and 70 % ZrO₂ + 30 % CaO. Fifteen hardness measurements were made on the cross-sections of the samples, six measurements were made on the specific external coating (C), three on the primer coating (B) and six on the base material (A), in the micro-areas marked in Figure 3. The results of the measurements are presented in Tables 3 and 4.

Table 4: Results of the hardness measurement on the cross-section of the sample after spraying it with 70 % ZrO₂ + 30 % CaO powder

Tabela 4: Rezultati meritve trdote na preseku vzorca po napršenem nanosu prahu iz 70 % ZrO₂ + 30 % CaO

| Test area | Test point | Load (N) | HV hardness |
|--|------------|----------|-------------|
| External coating (C) (70 % ZrO ₂ + 30 % CaO) | 1 | 5.0 | 705 |
| | 2 | 5.0 | 479 |
| | 3 | 5.0 | 549 |
| | 4* | 5.0 | 1176 |
| | 5 | 5.0 | 961 |
| | 6 | 5.0 | 449 |
| Primer coating (B) (Ni-Al-Mo) | 7 | 0.1 | 446 |
| | 8 | 0.1 | 397 |
| | 9 | 0.1 | 380 |
| Substrate material (A) (S235JR) | 10 | 0.5 | 231 |
| | 11 | 0.5 | 209 |
| | 12 | 0.5 | 245 |
| | 13 | 0.5 | 140 |
| | 14 | 0.5 | 126 |
| | 15 | 0.5 | 127 |

* The hardness measured on oxide precipitates with a larger area

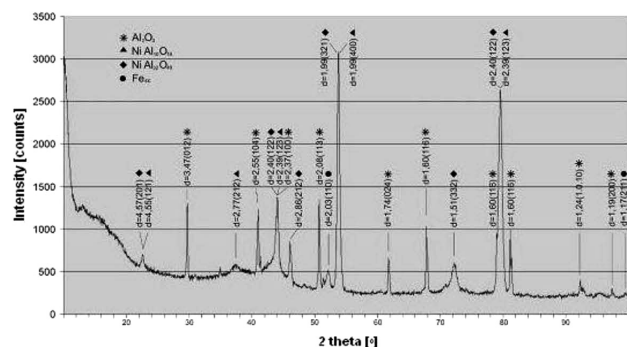


Figure 4: Diffraction pattern of the coating flame-sprayed with 97 % Al₂O₃ + 3 % TiO₂ powder

Slika 4: Rentgenogram plamensko nanešenega nanosa iz prahu s 97 % Al₂O₃ + 3 % TiO₂

A. CZUPRYŃSKI: PROPERTIES OF $\text{Al}_2\text{O}_3/\text{TiO}_2$ AND ZrO_2/CaO FLAME-SPRAYED COATINGS

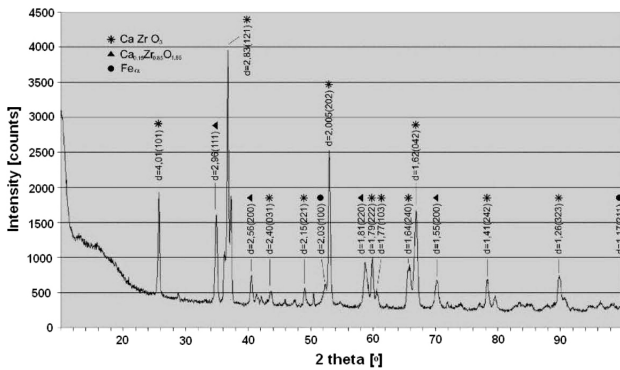


Figure 5: Diffraction pattern of the coating flame-sprayed with 70 % ZrO_2 + 30 % CaO powder
Slika 5: Rentgenogram plamensko nanešenega nanosa iz prahu s 70 % ZrO_2 + 30 % CaO

X-ray structure tests of the surfaces of the samples after flame spraying made with an X-ray diffractometer enabled us to determine the phase compositions of the external specific surfaces including the powders of aluminium oxide and zirconium oxide on the substrate of the primer coating created using the Ni-Al-Mo powder and the base material of the S235JR low-carbon steel. The results of the X-ray qualitative analysis are shown with diffraction patterns (Figures 4 and 5). Exact examinations of the structures of the coatings were carried out with an electronic scanning microscope. Metallographic microsections were viewed with a magnification of 250–5000 \times . The results of the examinations with the scanning microscope allowed us to determine the influence of the type of the powder used in the spraying

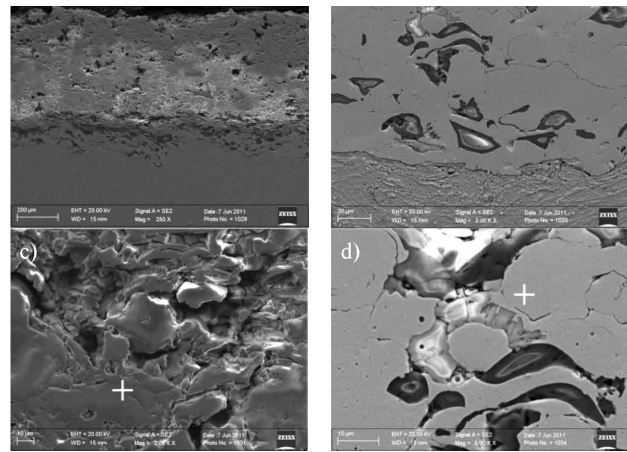


Figure 7: View of the coating after flame spraying 70 % ZrO_2 + 30 % CaO powder: a) external coating with a small amount of hollows, b) primer coating, c) structure of external coating, d) area of primer coating

Slika 7: Izgled nanosa po plamenskem nanašanju prahu s 70 % ZrO_2 + 30 % CaO : a) zunanji nanos z majhnim deležem praznin, b) osnovni nanos, c) struktura zunanjega nanosa, d) področje osnovnega nanosa

process on the structure of an external specific coating and the concentration of the elements in the selected micro-areas. The examples of observing the microstructures of the external coating and the primer coating are shown in Figures 6 and 7.

An abrasive-wear-resistance test of the mineral-mineral type of coatings involving the selected powders was performed on samples with dimensions of 5 mm \times 25 mm \times 75 mm in line with ASTM G65. The weight wear of a sample was determined as a result of the test, found after (100, 125, 250, 500 and 1500) revolutions of an abrasive pressure plate. The tests results allowed us to determine the abrasive-wear resistance of the deposited coatings. The measurement results of the abrasive-wear-resistance tests are presented in Table 5.

An erosion-resistance test was carried out in accordance with ASTM G76-95 on the samples with dimensions of 5 \times 25 \times 75 mm with the coatings involving the powders of 97 % Al_2O_3 + 3 % TiO_2 and 70 % ZrO_2 + 30 % CaO . Aluminium oxide (Al_2O_3) powder with a particle diameter of 45–70 μm was used as the erosion material. The test was undertaken at a molecular velocity of 70 \pm 2 m/s, an erodent flow rate of approx. 2 g/min, a nozzle outlet-to-sample distance of 10 mm and incidence angles of the abrasive stream of (90, 60, 30 and 15) $^\circ$. The test lasted for 10 min. The results are presented in Table 6.

The coating-adhesion test R_h (the stripping strength) was determined with the stripping method involving a static tensile test, in accordance with EN 582:1996, on cylindrical samples with a diameter of ϕ 40 mm, flame-sprayed with the powders containing 97 % Al_2O_3 + 3 % TiO_2 and 70 % ZrO_2 + 30 % CaO . The face of a cylindrical sample with a coating deposited was bonded to the counter specimen with the Henkel Loctite Hysol 3478 A&B Superior Metal bonding agent with a tensile

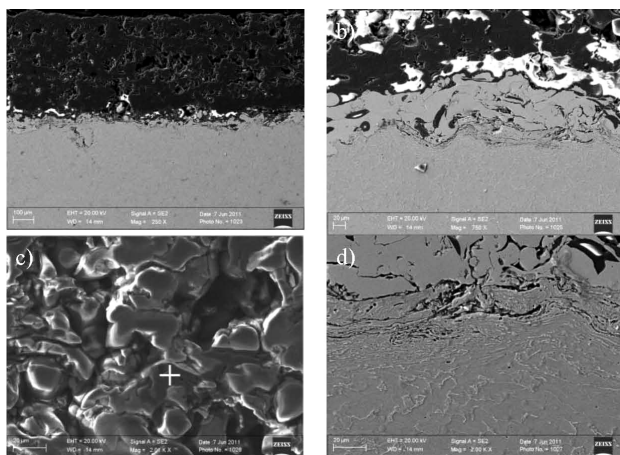


Figure 6: View of the coating after flame spraying 97 % Al_2O_3 + 3 % TiO_2 powder: a) structure of external coating with primer coating and base material with visible hollows of a varied size in the external coating of the sample; b) small amount of hollows in the external coating in the border area with primer coating; c) structure of external coating; d) area of base material and primer coating

Slika 6: Izgled nanosa po plamenskem nanašanju prahu s 97 % Al_2O_3 + 3 % TiO_2 : a) struktura zunanjega nanosa z nanosom podlage in osnovnim jeklom, z različnimi vidnimi prazninami različne velikosti v zunanjem nanosu vzorca, b) malo praznin v zunanjem nanosu na mejnem področju z osnovnim nanosom, c) struktura zunanjega nanosa, d) področje osnovnega jekla in osnovnega nanosa

Table 5: Results of the wear tests for the coatings made of 97 % Al_2O_3 + 3 % TiO_2 powder and 70 % ZrO_2 + 30 % CaO powder

Tabela 5: Rezultati preizkusov obrabe napršenih nanosov s prahom s 97 % Al_2O_3 + 3 % TiO_2 in 70 % ZrO_2 + 30 % CaO

| Powder composition | Sample No. | Revolutions (n) | Test No. | Sample weight prior to the test (g) | Sample weight after the test (g) | Mass loss (g) | Average mass loss (g) | Volume loss (mm^3) |
|--|------------|-----------------|----------|-------------------------------------|----------------------------------|---------------|-----------------------|-------------------------------|
| 97% Al_2O_3 + 3% TiO_2 | S 1.1 | 1500 | 1 | 75.8406 | 75.0086 | 0.8320 | 0.8314 | 207.85 |
| | | | 2 | 75.8396 | 75.0086 | 0.8310 | | |
| | | | 3 | 75.8395 | 75.0084 | 0.8311 | | |
| | S 1.2 | 500 | 1 | 75.0825 | 74.6428 | 0.4397 | 0.4387 | 109.66 |
| | | | 2 | 75.0821 | 74.6431 | 0.4390 | | |
| | | | 3 | 75.0802 | 74.6427 | 0.4375 | | |
| | S 1.3 | 250 | 1 | 75.4531 | 75.2617 | 0.1914 | 0.1840 | 92.00 |
| | | | 2 | 75.4524 | 75.2618 | 0.1906 | | |
| | | | 3 | 75.4517 | 75.2816 | 0.1701 | | |
| | S 1.4 | 125 | 1 | 75.8165 | 75.6092 | 0.2073 | 0.2074 | 51.85 |
| | | | 2 | 75.8164 | 75.6091 | 0.2073 | | |
| | | | 3 | 75.8167 | 75.6094 | 0.2073 | | |
| | S 1.5 | 100 | 1 | 73.8637 | 73.7352 | 0.1285 | 0.1283 | 32.07 |
| | | | 2 | 73.8635 | 73.7351 | 0.1284 | | |
| | | | 3 | 73.8634 | 73.7355 | 0.1279 | | |
| 70% ZrO_2 + 30% CaO | S 2.1 | 250 | 1 | 74.7266 | 74.0916 | 0.6350 | 0.6347 | 112.34 |
| | | | 2 | 74.7263 | 74.092 | 0.6343 | | |
| | | | 3 | 74.7262 | 74.0915 | 0.6347 | | |
| | S 2.2 | 500 | 1 | 77.6013 | 76.638 | 0.9633 | 0.9633 | 170.49 |
| | | | 2 | 77.6014 | 76.6378 | 0.9636 | | |
| | | | 3 | 77.6012 | 76.6381 | 0.9631 | | |
| | S 2.3 | 1500 | 1 | 76.9207 | 75.458 | 1.4627 | 1.4626 | 258.87 |
| | | | 2 | 76.9205 | 75.4578 | 1.4627 | | |
| | | | 3 | 76.9206 | 75.4581 | 1.4625 | | |
| | S 2.4 | 125 | 1 | 76.8146 | 76.1956 | 0.6190 | 0.6190 | 109.56 |
| | | | 2 | 76.8148 | 76.1954 | 0.6194 | | |
| | | | 3 | 76.8143 | 76.1958 | 0.6185 | | |
| | S 2.5 | 100 | 1 | 78.5391 | 77.8907 | 0.6484 | 0.6485 | 114.78 |
| | | | 2 | 78.5394 | 77.8905 | 0.6489 | | |
| | | | 3 | 78.5391 | 77.891 | 0.6481 | | |

Table 6: Mass-loss values in erosion tests for the coatings made of 97% Al_2O_3 +3% TiO_2 and 70% ZrO_2 +30% CaO powders

Tabela 6: Vrednosti masne izgube pri erozijskem preizkusu napršenega nanosa iz prahov s 97 % Al_2O_3 + 3 % TiO_2 in 70 % ZrO_2 + 30 % CaO

| Erodent incidence angle (°) | Type of powder sprayed | | | | | |
|-----------------------------|---|--------------------------------|---------------|---|--------------------------------|---------------|
| | 97 % Al_2O_3 + 3 % TiO_2 | | | 70 % ZrO_2 + 30 % CaO | | |
| | Sample mass prior to the test (g) | Sample mass after the test (g) | Mass loss (g) | Sample mass prior to the test (g) | Sample mass after the test (g) | Mass loss (g) |
| 90° | 73.8752 | 73.8703 | 0.0049 | 75.9886 | 75.9560 | 0.0026 |
| 45° | 73.8703 | 73.8485 | 0.0218 | 75.9560 | 75.9118 | 0.0442 |
| 30° | 73.8485 | 73.8206 | 0.0279 | 75.9118 | 75.8640 | 0.0378 |
| 15° | 73.8206 | 73.8027 | 0.0179 | 75.8640 | 75.8020 | 0.0620 |

Table 7: Results of the adhesion tests for the coatings made of 97 % Al_2O_3 + 3 % TiO_2 and 70 % ZrO_2 + 30 % CaO powders

Tabela 7: Rezultati adhezijskih preizkusov nanosov napršenih s prahovi s 97 % Al_2O_3 + 3 % TiO_2 in 70 % ZrO_2 + 30 % CaO

| Material of the external coating | Sample No. | Sample size | | Maximum breaking load (N) | Adhesion of sprayed coating (N/mm^2) | |
|--|------------|----------------------|---------------------------------------|---------------------------|--|---------------|
| | | Sample diameter (mm) | Cross-section field (mm^2) | | R_h | $R_{h Av.}^*$ |
| | | | | | | |
| 97 % Al_2O_3 + 3 % TiO_2 | 1/1 | 39.4 | 1218.6 | 7614.0 | 6.0 | 6.5 |
| | 1/2 | 39.0 | 1193.9 | 6418.0 | 5.4 | |
| | 1/3 | 39.8 | 1243.5 | 10095.0 | 8.1 | |
| 70 % ZrO_2 + 30 % CaO | 2/1 | 39.8 | 1243.5 | 4104.0 | 3.3 | 3.3 |
| | 2/2 | 39.8 | 1243.5 | 4376.0 | 3.5 | |
| | 2/3 | 39.5 | 1224.8 | 3735.0 | 3.1 | |

* average value

strength of 17 MPa. The samples, together with the fixing device, were placed in a tensile-testing machine and subjected to static stretching until rupture. Tensile test results allowed us to determine the values of the force detaching the coatings from the substrate and calculate the adhesion coefficient (Table 7).

A thermal-resistance test was carried out, in line with ISO 14923:2003, on the samples with the dimensions of $5 \times 25 \times 75$ mm with an external coating including 97 % $\text{Al}_2\text{O}_3 + 3\%$ TiO_2 and an external flame-sprayed coating including 70 % $\text{ZrO}_2 + 30\%$ CaO . Three stages of the test were determined as no detailed guidance concerning this type of test was available:

- the first stage – heating to 1050 °C and slow cooling, together with the oven, at a rate of 40 °C/h;
- the second stage – heating to 1050 °C and cooling the samples in a stream of compressed air at a rate of 25 °C/s, the cycle was repeated ten times;
- the third stage – heating to 1050 °C and a rapid cooling of the samples in water at a rate of 100 °C/s. The test result identified the number of the cycle, after which discontinuities and delamination were visible on the coating surface (Figure 8).

3 DISCUSSION

After carrying out the spraying process, the visual examinations did not reveal any sample-surface imperfections after flame spraying the 97 % $\text{Al}_2\text{O}_3 + 3\%$ TiO_2 and 70 % $\text{ZrO}_2 + 30\%$ CaO powders. The metallographic examinations of the microsections perpendicular to the surface of the sample sprayed with the 97 % $\text{Al}_2\text{O}_3 + 3\%$ TiO_2

TiO_2 powder showed that two coatings existed on the surface of the steel, with a developed surface line: the primer coating (B) and the external specific coating (C) (Figure 1a). The 30–110 μm primer coating (B) consisted of bright areas made of the Ni-Al-Mo alloy and dark oxide inclusions (Figure 1c); it was observed immediately above the base-material surface (A). A banded structure of the base material, distinctive for the strengthening of the steel surface during the shot blasting of the examined material, existed in the boundary area, along the primer coating. The external coating, sprayed on the first buffer coatings, had a thickness varying between 450 μm to 510 μm . The coating exhibited numerous voids with different sizes and a waved line of its external surface (Figure 1d).

After the flame spraying of the steel surface with the 70 % $\text{ZrO}_2 + 30\%$ CaO powder, the following individual layers were identified: the primer coating (B) and the external specific coating (C) (Figure 2a). A banded structure with a considerable plastic deformation, existing on the thickness of approx. 50 μm , was observed underneath the primer coating, in the steel. The primer coating consisted of bright areas of the elements forming the Ni-Al-Mo powder used for spraying and also of dark flattened oxides (Figure 2c). The coating was 50–160 μm thick. The external specific coating of about 600 μm exhibited numerous voids with a developed line of its external surface (Figure 2d).

The specific external coating sprayed with the 97 % $\text{Al}_2\text{O}_3 + 3\%$ TiO_2 powder had a hardness of 671.8–909.9 HV5. The hardness of the examined micro-areas in the primer coating was lower, i.e., 353–469 HV01. The hardness of the substrate material in the boundary zone along the primer coating was approx. 226 HV05, as confirmed by the occurrence of a narrow heat-affected zone (HAZ) or by steel-surface strengthening after shot blasting. The hardness of the external specific coating after the flame-spraying operation involving the 70 % $\text{ZrO}_2 + 30\%$ CaO powder was different, ranging from approx. 449–961 HV5. The hardness measured on oxides with a larger area in the coating, in the places where oxide precipitates occurred, was even more than 1176 HV5. Different hardness results were due to a large number of voids in the coating. The hardness of the primer coating was from approx. 380 to approx. 446 HV01, and for the primer material, it was between 109–230 HV05.

X-ray structure tests allowed us to identify the phases existing in the structure of the coating after the flame spraying involving the 97 % $\text{Al}_2\text{O}_3 + 3\%$ TiO_2 and 70 % $\text{ZrO}_2 + 30\%$ CaO powders (Figures 4 and 5). There were mainly Al_2O_3 , $\text{NiAl}_{10}\text{O}_{16}$ and $\text{NiAl}_{32}\text{O}_{49}$ phases; trace amounts of Fe- α were also identified after the spraying operation resulting in the external coating with an aluminium matrix (Figure 4). The examinations did not show any presence of a phase with titanium in this coating due to its small amount in the content of the powder for spraying ($\text{TiO}_2 = 3\%$). The phase can be

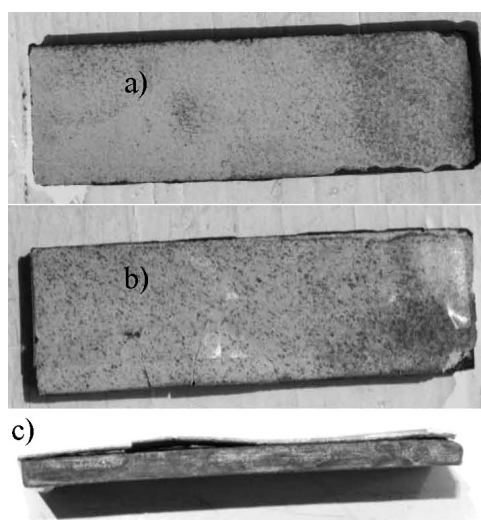


Figure 8: View of samples after the third stage of thermal-resistance tests: a) surface of the sample sprayed with 97 % $\text{Al}_2\text{O}_3 + 3\%$ TiO_2 powder, b) cracks on the surface of the coating made of 70 % $\text{ZrO}_2 + 30\%$ CaO powder, c) delamination of the coating made of 70 % $\text{ZrO}_2 + 30\%$ CaO powder

Slika 8: Izgled vzorcev po tretji stopnji preizkusa toplotne odpornosti: a) površina vzorca z nanosom prahu s 97 % $\text{Al}_2\text{O}_3 + 3\%$ TiO_2 , b) razpoke na površini nanosa prahu s 70 % $\text{ZrO}_2 + 30\%$ CaO , c) odstopanje nanosa iz prahu s 70 % $\text{ZrO}_2 + 30\%$ CaO od površine

identified with X-ray tests, provided it exists in the amount of more than 4 % of mass fraction.

Ten diffraction lines from the Al_2O_3 phase were shown in the diffraction pattern, including the maximum intensity values for planes (113), (116), (124), (030) and (1.0.10). Four diffraction lines for planes (121), (212), (400) and (123) of the $\text{NiAl}_{10}\text{O}_{16}$ phase and for planes (201), (321), (332), (122) of the $\text{NiAl}_{32}\text{O}_{49}$ oxide phase were also found. The existence of diffraction lines (100) and (211) with a small intensity, relating to Fe- α , was also confirmed. The presence of compound zirconium and calcium oxides was also revealed in the structure of the external surface obtained after the spraying operation involving the 70 % ZrO_2 + 30 % CaO powder. Ten peaks relating to the planes of the CaZrO_3 phase and four peaks relating to the planes of the $\text{Ca}_{0.15}\text{Zr}_{0.85}\text{O}_{1.85}$ phase occur in a diffraction pattern (**Figure 5**). The existence of peaks with a small intensity for planes (100) and (211), derived from the Fe α steel surface, was also found.

The results of the wear-resistance test allowed us to conclude that the flame-sprayed 97 % Al_2O_3 + 3 % TiO_2 coating was more resistant than the coating made with the 70 % ZrO_2 + 30 % CaO powder within the tested range of revolutions of 100–1500 (**Table 5**).

It was confirmed, based on erosion-resistance tests, that the coating made with the 97 % Al_2O_3 + 3 % TiO_2 powder exhibits a higher erosion resistance (determined with the mass loss) than the coating made with the 70 % ZrO_2 + 30 % CaO powder, except in the case of testing it at the angle of 90°. In the cases of the erosion tests at the angles of (45, 30 and 15)°, the mass loss of the sample with the 93 % Al_2O_3 + 3 % TiO_2 coating was 0.0218, 0.0279 and 0.0179 g, respectively, while for the sample with the 70 % ZrO_2 + 30 % CaO coating, it was higher by about 50 % (**Table 6**).

The substrate adherence of the flame-sprayed coatings made with the 97 % Al_2O_3 + 3 % TiO_2 and 70 % ZrO_2 + 30 % CaO powders, determined with a static-stretching test, involving a detachment of the coating from the substrate, showed that the adherence of the coating made of the 97 % Al_2O_3 + 3 % TiO_2 powder was higher than that of the coating made of the 70 % ZrO_2 + 30 % CaO powder, being 6.5 MPa and 3.3 MPa, respectively (**Table 7**). The difference between the tensile-strength and adhesion values was confirmed by inhomogeneous microsections of the samples' surfaces after the tensile test.

The thermal resistance was investigated with the method of cyclic heating the samples coated on one side with the 97 % Al_2O_3 + 3 % TiO_2 coating and 70 % ZrO_2 + 30 % CaO coating to 1050 °C and cooling them down at rates of 40 °C/h (in an oven), 25 °C/s (air cooling) and 100 °C/s (water cooling). After heating the samples to 1050 °C and cooling them down using an oven in the first cycle of the test, compressed air in the next nine cycles and water after the last cycle, the coating made of the 70 % ZrO_2 + 30 % CaO powder delaminated from

the substrate and cracks were identified on it, along with the detached coating (**Figure 8c**). No damages in the form of delamination were identified for the coating made of the 97 % Al_2O_3 + 3 % TiO_2 powder; however, small cracks without broken-out sections were recorded (**Figure 8a**).

4 CONCLUSIONS

The following conclusions were formulated based on the investigations performed and the outcomes obtained and analysed:

1. Flame spraying with the 97 % Al_2O_3 + 3 % TiO_2 and 70 % ZrO_2 + 30 % CaO powders carried out within the range of the selected parameters allowed us to achieve high-quality ceramic coatings of approx. 500 μm applied to a steel substrate.
2. The structure of the coating flame-sprayed with the 97 % Al_2O_3 + 3 % TiO_2 powder consisted mainly of aluminium oxide and a small amount of the $\text{NiAl}_{10}\text{O}_{16}$ and $\text{NiAl}_{32}\text{O}_{49}$ phases, while the coating made of the 70 % ZrO_2 + 30 % CaO powder showed a structure of oxide zirconium phases with calcium.
3. The bonding of the primer coating made of the Ni-Al-Mo powder with the steel substrate and of the external coatings made of the 97 % Al_2O_3 + 3 % TiO_2 and 70 % ZrO_2 + 30 % CaO powders was of the mechanical adhesion nature. The ceramic coatings including the aluminium-matrix powder and zirconium-matrix powder were characterised by their adhesion to the substrate, being 6.5 MPa and 3.3 MPa, respectively.
4. The coatings achieved, consisting of the 97 % Al_2O_3 + 3 % TiO_2 powder and 70 % ZrO_2 + 30 % CaO powder, exhibited the average hardness values of approx. 780 and approx. 720 HV, respectively.
5. The abrasive-wear resistance of the coating made of the 97 % Al_2O_3 + 3 % TiO_2 powder was higher than the resistance of the coating made of the 70 % ZrO_2 + 30 % CaO powder, and the average erosion-wear resistance for an erodent incidence angle of less than 90° was higher by approx. 50 %.
6. The coating made of the 97 % Al_2O_3 + 3 % TiO_2 powder exhibited cyclical-heat-stroke resistance, while the coating made of the 70 % ZrO_2 + 30 % CaO powder, heated and cooled in the same conditions, revealed cracks, chippings and delamination.

5 REFERENCES

- ¹ D. Janicki, High Power Diode Laser Cladding of Wear Resistant Metal Matrix Composite Coatings, *Solid State Phenomena, Mechatronic Systems and Materials V*, 199 (2013), 587–592, doi:10.4028/www.scientific.net/SSP.199.587
- ² A. Arcondéguy, G. Gasgnier, G. Montavon, B. Pateyron, A. Denoir-jean, A. Grimaud, C. Hugué, Effects of spraying parameters onto flame-sprayed glaze coating structures, *Surface and Coatings Technology*, 202 (2008), 4444–4448

A. CZUPRYŃSKI: PROPERTIES OF Al₂O₃/TiO₂ AND ZrO₂/CaO FLAME-SPRAYED COATINGS

- ³ A. Lisiecki, Titanium Matrix Composite Ti/TiN Produced by Diode Laser Gas Nitriding, *Metals - Open Access Metallurgy Journal*, 5 (2015) 1, 54–69, doi:10.3390/met5010054
- ⁴ D. Janicki, Disk Laser Welding of Armor Steel, *Archives of Metallurgy and Materials*, 59 (2014), 1641–1646, doi:10.2478/amm-2014-0279
- ⁵ A. Lisiecki, Welding of Thermomechanically Rolled FineGrain Steel by Different Types of Lasers, *Archives of Metallurgy and Materials*, 59 (2014), 1625–1631, doi:10.2478/amm-2014-0276
- ⁶ A. Kurc-Lisiecka, W. Ozgowicz, W. Ratuszek, J. Kowalska, Analysis of deformation texture in AISI 304 steel sheets, *Solid State Phenomena*, 203–204 (2013), 105–110, doi:10.4028/www.scientific.net/SSP.203-204.105
- ⁷ M. Adamiak, L. A. Dobrzański, Microstructure and selected properties of hot-work tool steel with PVD coatings after laser surface treatment, *Applied Surface Science*, 254 (2008) 15, 4552–4556
- ⁸ L. A. Dobrzański, M. Adamiak, Structure and properties of the TiN and Ti(C,N) coatings deposited in the PVD process on high-speed steels, *Journal of Materials Processing Technology*, 133 (2003), 50–62
- ⁹ J. Górka, Weldability of Thermomechanically Treated Steels, Having a High Yield Point, *Archives of Metallurgy and Materials*, 60 (2015), 469–475, doi:10.1515/amm2015-0076
- ¹ A. Czupryński, J. Górka, M. Adamiak: Examining properties of arc sprayed nanostructured coatings, *Metalurgija*, 55 (2016) 2, 173–176
- ¹⁰ L. Pawlowski, *The Science and Engineering of Thermal Spray Coatings*, second ed., John Wiley & Sons, Chichester, UK, 2008
- ¹¹ K. Spencer, M. X. Zhang, Heat treatment of cold spray coatings to form protective intermetallic layers, *Scripta Materialia*, 61 (2009), 44–47
- ¹² F. Vargas, H. Ageorges, P. Fournier, P. Fauchais, M. E. López, Mechanical and Tribological Performance of Al₂O₃-TiO₂ Coatings Elaborated by Flame and Plasma Spraying. *Surface and Coatings Technology*, 205 (2010), 1132–1136, doi:10.1016/j.surfcoat.2010.07.061